

Fitting avalanche-dynamics models with documented events from the Col du Lautaret site (France) using the conceptual approach

Maurice Meunier, Christophe Ancey, & Jean-Michel Taillandier^{a,b,a}

^a*Cemagref, unité Erosion Torrentielle, Neige et Avalanches, Domaine Universitaire, 38402 Saint-Martin-d'Hères Cedex, France*

^b*École Polytechnique Fédérale de Lausanne, Laboratoire d'Hydraulique Environnementale, Ecublens, 1015 Lausanne, Switzerland*

Abstract

This paper tests three conceptual avalanche-dynamics models by comparing their predictions to 14 documented avalanches observed at the Lautaret Pass (France). Three models were used: the Voellmy-like model, an extension of this model (referred to as the generalized Voellmy-like model), and a new model deduced, referred to as the modified Coulomb-like model. Compared to deterministic physically-based models, these models are not intended to describe the dynamical behavior of avalanches, but to mimic their behavior by using nonlinear mathematical operators. Agreement between model predictions and field data was uneven: the three models succeeded in reproducing the run-out distance, but only two of them (generalized Voellmy and Coulomb-like models) provided correct estimates of avalanche velocity.

Key words: Avalanche dynamics; conceptual model; experimental field site; fitting

1 Introduction

In this paper a series of documented avalanches is used to fit conceptual avalanche-dynamics models. This work is motivated by the two following points:

- Rheological equations used so far in avalanche-dynamics models are speculative. The rheology of flowing snow include very complex processes, e.g. the rheological properties may vary from one event to another because of meteorological conditions; when the avalanche goes down, snow properties can alter as a result of snow compression, snowball formation (increase in

water content), air entrainment, etc.; neighboring paths can produce very different avalanches because of the relief influence. This large variability in snow properties can lead to thinking that the current avalanche-dynamics models are not physically based, but instead should be considered as conceptual models. This is consistent with the fact that their parameters are never measured, but fitted. This is the idea that we will further explore here. In a companion paper (Meunier and Ancey, 2004), we have developed a conceptual model (this notion will be explained later) and shown its interest in modeling extreme snow avalanches.

- Most avalanche-dynamics models introduce two friction parameters in the rheological equation. These two parameters have been adjusted by using field data; usually a single type of measurement (e.g. the run-out distance) is available. Typical examples include the following ones: Schaerer (1974) used the velocities in the part of the profile where a steady state was expected to occur (for 47 measurements taken from 21 different paths). Bakkehøi et al. (1980) used runout distances from 136 paths. Buser and Frutiger (1980) used the runout distances of 10 extreme avalanches on 10 paths. All these researchers wanted to determine two friction parameters, but they could use a single type of measurement. They overcame this difficulty by using *ad hoc* assumptions: Schaerer (1974) used a relationship between the Coulombic friction coefficient μ and avalanche velocity; Buser and Frutiger (1980) assumed that the friction parameters (μ, ξ) of the Voellmy model are the same for all the events. Bakkehøi et al. (1980) did not solve the problem and gave a practical range of the two parameters $(\mu, M/D)$, where M is the mass of the avalanche and D is the drag coefficient. In contrast, here we will consider a series of events for which both the velocity and run-out distances were recorded. This makes it possible to adjust the friction parameters more properly. Note that, except for the work done by Gubler et al. (1986) and Gubler (1987), there are not many attempts to properly adjust two-parameter avalanche-dynamics models.

This paper will attempt to fit three two-parameter models. The adjustment procedure will be conducted by using the conceptual approach, i.e., we will not use any physical argument in adjusting the models or in interpreting the results. First, we will present the conceptual approach from a theoretical point of view, with focus on avalanche-dynamics models. Then the field site of Col du Lautaret and the recorded data will be described. We will show that simple linear models fail to reproduce the output data, which include the run-out distance and the velocity measured at one point of the path profile. Finally, three conceptual models will be presented and tested against field data.

2 The conceptual approach

Avalanches are natural phenomena that can be studied within the framework of fluid mechanics, but the same scientific methodology as water (e.g. for floods) cannot be used because of the complexity of snow properties and scale effects between full-scale avalanches and laboratory experiments. Despite these issues, most researchers still think that avalanche dynamics should be dealt with by using a deterministic framework [e.g. Harbitz et al. (1998)]. Most avalanche-dynamics models use a rheological equation, which can be broken down into two contributions: a Coulombic contribution and a turbulent contribution, giving rise to the Voellmy model of the frictional force. No clear evidence has been provided so far to justify this model. On the contrary, the recent investigation by Ancey and Meunier (2004) reveals that the dependence of the frictional force on avalanche velocity is much more complex than assumed by Voellmy's assumption. Given the difficulties met in describing avalanche dynamics, an alternative approach is to idealize the avalanche motion by using a conceptual approach similarly to the longstanding practice in hydrology [e.g., see (O'Connell and Todini, 1996)].

The basic idea is to assume that there is a single functional relationship G between the two output variables (run-out distance and velocity at one point) and other field data. These other field data include snowfalls preceding the avalanche, starting point elevation, released snow volume, etc. For the moment, we do not specify the type and number of these data but merely refer to them generically as the input variables Θ . The functional relationship G relates the output variables Ω of a given event to the input variables Θ . Obviously there is not a one-to-one universal function linking Ω to Θ : indeed, it is expected that G also depends on the topographical features of the path and on a set Π of internal or structural parameters, reflecting the diversity and variability of snow properties and avalanche motion:

$$\Omega = G(\Theta|\Pi, \text{path}).$$

Here, in order to take the path influence into account, we assume that the functional G is a mathematical operator resulting from the integration of a momentum equation along the path profile $z = f(x)$ (see below). In this paper, since we will use only the experimental events obtained on the Lautaret field site; the run-out distance x_{stop} and the maximum velocity measured in one point u_{obs} are the output variables: $\Omega = \{x_{stop}, u_{obs}\}$ for the three models. Furthermore, the input variables Θ and the internal parameters Π will depend on the chosen model.

At the risk of blurring the border between the conceptual and physical approaches, it seems natural to use operators based on fluid-mechanics equations, i.e., based on either partial derivative or differential equations describing the

fluid motion. As the partial derivative equations of the fluid flows require a great deal of input data (boundary and initial conditions), which are rarely available, the simplest models are based on the differential equation used to calculate the movement of a block sliding on a slope. In order to integrate the momentum equation along the path profile, an avalanche is idealized as a solid mass sliding along a curvilinear path and experiencing a frictional force F , possibly depending on θ and/or u (θ is the local slope, u is the local velocity). We assume that the structure of this frictional force is identical whatever the path and the avalanche; only its parameters can vary from one event to another. The three models differ only in the model used for the frictional force F . Here we will consider: $F = \mu mg \cos \theta + \kappa u^2$ (Voellmy-like model, § 5.1), $F = \mu(x)mg \cos \theta + \kappa(x)u^2$ (generalized Voellmy-like model, § 5.2), and $F = kmg \cos \theta (\tan \theta - \mu)$ (modified Coulomb-like model, § 5.3). The general expression of the momentum equation can be written:

$$\frac{du}{dt} = g \sin \theta - \frac{F(\theta, u)}{m}, \quad (1)$$

where m is the avalanche mass and t is time. As initial conditions, we use $u(x_{start}) = 0$, where x_{start} is the starting-point abscissa. The momentum equation is integrated along the path profile $z = f(x)$, where z denotes the elevation and x the abscissa along a horizontal axis; s is a curvilinear abscissa taken from an arbitrary origin on the path profile: $s = \int_0^s (1 + f'^2(\sigma))^{-1/2} d\sigma$. After integrating the equation numerically, we look for the two output variables of interest: the run-out distance x_{stop} is given by the position of the stopping point at which the avalanche velocity vanishes, the maximum velocity calculated at the abscissa of the measuring mast is stored. If they differ from the experimental output variables, we modify the internal parameters Π until experimental and calculated values compare sufficiently. As Equation 1 is used as the basis for the conceptual models and not in a deterministic approach, we will call the conceptual models Voellmy-like or Coulomb-like models in order to distinguish them from the deterministic models.

3 Lautaret field site

4 The available data

The Lautaret field site (see Fig. 1) is located on a southeast slope between 2000 and 2400 m in elevation. Figure 2 shows the profile of the two main paths. In the 1970s, avalanches were released with explosives. The starting elevation of these releases was approximately the same for all avalanches ($Z_{start}=2330$ – 2335 m for Path 1 and $Z_{start} = 2380$ – 2385 m for Path 2). The researchers who

conducted the experiments used a map at the scale of 1:5000 and gave the starting and stopping (Z_{stop}) elevations within an uncertainty of ± 1 m. Since they reported their measurements in terms of run-out elevation, we followed them and used this datum rather than the abscissa x , even though z is less relevant in practice. Several masts were installed perpendicular to the slopes (at $z = 2227$ m for Path 1 and $z = 2225$ m for Path 2; see Fig. 2). Pressure and velocity sensors were mounted on the masts. Pressure sensors were membrane sensors or dynamical sensors; punctual velocity was measured with propeller-type Nerflux probes provided by Neyrtec (France). The avalanche front speed was measured by using photogrammetry techniques. Further information can be found in (Bon Mardion et al., 1975) and (Eybert-Bérard et al., 1977, 1978). The uncertainty of the velocity was estimated by the investigators to lie in the range 5–10%; here we adopt $\pm 10\%$. Other measurements were taken: density of the snow in motion as well as density and temperature in the snowcover in the starting area (before the release) and in the avalanche deposits. Density measurements were taken by using gamma densitometry techniques. For each experiment, ram tests and stratigraphic profiles were done. The avalanche depth was estimated from the number of sensors on the masts affected by the avalanche.

Twenty-two events were recorded for Path 1 and Path 2 (Eybert-Bérard et al., 1978). However, not all the events were fully documented. Eventually, we had nine events versus fourteen for Path 1 and five versus eight for Path 2. These events are reported in boldface in Table 1. The volumes of the avalanches were rather small (500–1500 m³). The run-out distances varied from 300 to 800 m. Table 2 reports three types of avalanches with the corresponding snow type. The first type is a dense avalanche composed of powder snow and should not be confused with an airborne avalanche. The avalanche phenomenon was analyzed by Eybert-Bérard et al. (1978): “for the two first types, there is always a dense snow flowing at the bottom and a powder cloud on the top. This powder cloud is more important when the density is smaller and the snow colder. Wet snow, characteristic of the third type, gives a slower flow made of dense flowing snow without any powder cloud.” The authors also remarked the tendency of the flowing snow to become denser and warmer, especially in the stopping phase.

The available quantitative data (velocity, density, run-out distance, etc.) do not show noticeable differences between the three avalanche types when we examine these data one by one because their ranges of variation overlap widely. However, Eybert-Bérard et al. (1978) pointed that the first category behaved in a slightly different way: greater run-out distances, lower densities, and higher velocities. Figure 3 shows that this difference appears when combining the run-out distances and the measured velocities. As a consequence we separated the first type of avalanches from the two others.

Since velocity measurements obtained by photogrammetry and Nerflux probes were well correlated, it was possible to estimate some of the missing velocity values. All the data useful for the study are presented in Table 1. We used the velocity measurements provided by the Nerflux probes. When the avalanche flow depth could not be measured exactly, but only a minimum value was provided, we used this value in the computations.

4.1 *Are linear models pertinent?*

Figure 3 shows that there is no correlation between velocity and run-out distance, whereas we only found a slight correlation between velocities and flow depths (see Fig. 4). This is confirmed by the middle value of the coefficient of determination $R^2 = 0.51$ for the data taken from the two paths. This clearly shows the complexity of avalanche behavior, since a physically-based approach would have suggested that the higher the velocity, the longer the run-out distance. Since linear correlation fails to reproduce one variable when the other is known, linear models are not pertinent and it is necessary to use nonlinear models.

5 Three conceptual dynamic models

5.1 *The Voellmy-like model*

In this model, the frictional force F in Equation 1 is split into a slope-dependent term and a velocity-dependent term: $F = \mu mg \cos \theta + \kappa u^2$, where $\Pi = \{\mu, \kappa\}$ are the two internal parameters. The former contribution makes it possible to control the avalanche run-out distance, whereas the latter mainly influences the maximum velocity that the avalanche can reach. Moreover, it has often been thought that the avalanche mass or volume often influences the force: the larger volume V is, the lower its bulk friction is. Thus, parameter κ must be a function of the avalanche volume. For convenience, here we assume that this dependency can be written in the following form: $\kappa = g/(\xi H)$ where ξ is a friction coefficient and H is a typical length assumed to give an estimate of the flow depth of the avalanche. We will adopt the maximum avalanche flow depth measured at the mast. Finally, in this model, we have: $\Theta = \{x_{start}, H\}$. H as well as the internal parameters Π are considered constant all along the path profile.

Considered from a deterministic perspective, this model is well-known and often found in the literature (Bakkehøi et al., 1980; Buser and Frutiger, 1980;

Perla et al., 1980; Bakkehøi et al., 1983; Salm et al., 1990; Salm, 1993). As already stated, it has been fitted manifold, but most often by using incomplete data. Moreover, a back analysis on the bulk rheological behavior of a few documented events showed no square-velocity dependency (Ancy and Meunier, 2004). Lastly, it is already known that the Voellmy model gives underestimated velocity values in some cases (Bartelt et al., 1997). Let us examine the reasons why the Voellmy model can fail to be adjusted. To obtain a constant value for a single output variable (for instance x_{stop}), there is an infinity of solutions for the internal parameters Π , as shown in Fig. 5 for a given event observed in Lautaret Path 1. The corresponding calculated velocity $u_{calc}(\xi)$ has an asymptotic value; for other paths, velocity can reach a maximum value before decaying to its asymptotic value. Let us refer to it as u_{asympt} . If the measured value u_{obs} exceeds u_{asympt} , it is not possible to adjust Π . If it is lower but very close to u_{asympt} (see Fig. 5), the uncertainty of the solution for ξ will be very high because of the convexity of the curve $u_{calc}(\xi)$. In order to overcome this problem, we adopt the following criterion: $u_{obs} \leq 0.9u_{asympt}$ for Π to be determined. The factor 0.9 is arbitrary and accounts for the uncertainty on the measurements of u_{obs} .

5.2 The Generalized Voellmy-like model

Bartelt et al. (1997) solved the problem of underestimated velocity in the Voellmy model by assuming that the internal parameters Π can vary along the path profile: $\Pi(x) = \{\mu(x), \xi(x)\}$. We will refer to this model as the generalized Voellmy-like model.

The degree of freedom of this functional dependence is infinite. We want to reduce this degree of freedom by arbitrarily setting the functions of Π . For the Aulta path (Switzerland), Bartelt et al. (1997) linked $\xi(x)$ with $\mu(x)$ by using a relationship that can be approximated by: $\xi(x) = e^{10-6\mu(x)}$. We consider that this relation holds for the Lautaret paths for any type of avalanche. To relate $\mu(x)$ and $\tan \theta(x)$, we assume that

$$\mu(x) = \frac{\mu_{max} + \mu_{min}}{2} + \frac{\mu_{max} - \mu_{min}}{2} \tanh [R (\tan \theta_{moy} - \tan \theta(x))], \quad (2)$$

where μ_{min} and μ_{max} are the two bounds within which $\mu(x)$ can vary. Note that this equation holds for the Aulta path (see Fig. 6). The curve behavior is ruled by $\tan \theta_{moy}$ (shifting property) and by R (steepness property):

- for low and positive values of R , the curve is flat,
- for large and positive values of R , it decreases smoothly but rapidly from μ_{max} to μ_{min} when $\tan \theta(x)$ is close to $\tan \theta_{moy}$ for high values of R ,

- for negative R values, the curve varies inversely, i.e., $\mu(x)$ increases from μ_{min} to μ_{max} with increasing $\theta(x)$.

Since this function has four parameters, we must keep two of them constant in order to obtain two internal parameters for the fitting. After many attempts, we decided to set $\mu_{min} = 0.1$ and $\tan \theta_{moy} = 0.6$. Finally, for the internal parameters, we obtain $\Pi = \{\mu_{max}, R\}$. If μ_{min} and $\tan \theta_{moy}$ are conveniently chosen, we should be able to fit all the events with this generalized Voellmy-like model.

5.3 The modified Coulomb-like model

This model is also based on Equation 1, but the expression of the frictional force differs from the Voellmy model. Different observations drawn from the Aulta-avalanche behavior (see Fig. 7) justify this new model. Three phases in Fig. 7 can be recognized: (i) a starting and accelerating phase, (ii) a plateau phase where velocity varied in a smoother way than in the other phases, (iii) a quick decelerating and stopping phase (see also (Ancey and Meunier, 2004)). From the Aulta measured velocities, inverting Equation 1, we can deduce the values of the friction force $F(\theta, u)/m$ along the profile. This force varied slowly during the plateau. It was much lower in the accelerating phase, whereas it was higher in the decelerating phase. This means that the frictional force should depend on the sign of the acceleration. This dependence cannot be modeled with a friction force varying as a quadratic velocity such as the Voellmy-like equation, which explains why this model cannot calculate high velocities in certain cases.

The solution proposed here consists in using the Coulomb friction as the main friction force. When μ is properly chosen, the deviation between gravitational and frictional forces has the same sign as the acceleration: positive during the accelerating phase, but negative during the decelerating phase. We will amplify or decrease this deviation by introducing a new parameter k for the measured and calculated velocities to match. The equation of this new model is

$$\frac{du(x)}{dt} = kg \cos \theta(x) [\tan \theta(x) - \mu].$$

Note that this model is meaningless from the physical viewpoint (unless we try to interpret k as a mass-added coefficient or a factor reflecting avalanche mass balance), but is correct from the conceptual viewpoint. With $k > 1$, the difference between the gravity force and the frictional force increases and the velocity of the plateau phase should increase, and inversely when $k < 1$. The solution for the Aulta avalanche is obtained with $\mu = 0.4272$ and $k = 1.075$ (see Fig. 7). With this model we have $\Theta = \{x_{start}\}$ and $\Pi = \{\mu, k\}$. The flow depth of the avalanche is no longer an input variable.

This model has interesting properties:

- The equation of motion can be integrated along the path profile using the curvilinear abscissas s and analytical approximations can be proposed.
- The two internal parameters are independent coefficients: μ controls the run-out distance and k the velocities. In contrast with the Voellmy-like model, this model can be easily fitted by using the two output variables.
- The calculated velocities are proportional to \sqrt{k} ; this property can be used by practitioners when they have information on the velocity at one point to deduce the value of k and then calculate the velocities at any point. This also shows that the variation range of the computed velocity is $[0, \infty[$. There is no maximum limit contrary to the Voellmy-like model.
- This model is an extension of the Coulomb-like model with one parameter only, proposed for granular flows (Savage and Hutter, 1989) and used for avalanches (Mougin, 1922; Dent, 1993; Ancy, 2004). By setting $k = 1$, one can apply this model to paths where the only available output variable is the run-out distance (Ancy, 2004).

It will be necessary to test this new model on many examples to evaluate its confidence more precisely. Here, we will only fit the internal parameters $\Pi = \{\mu, k\}$ to the experimental results obtained on the Lautaret field site.

6 Results

6.1 The Voellmy-like model

The results are presented in Table 3. Only 50% of the events could be reproduced by using the Voellmy-like model. Failures occurred for every type of avalanches. Figure 8 reports the results in a diagram $x_{stop} - u_{obs}$: it is clearly seen that the adjustment procedure failed because recorded velocity measurements were higher than asymptotic velocities. We have plotted two border lines between the data scatters pertaining to fitted and not-fitted events. These borders depend on the avalanche path. On the contrary, when the results are reported in a diagram $u - \mu$ (see Fig. 9), we obtain the same border line for both paths, which is roughly parallel to the equation proposed by Schaerer (1974).

Finally, we conclude that the Voellmy-like model fits the results for only 50% of the events because of its limitation to compute high-velocity avalanches.

6.2 The generalized Voellmy-like model

All the events were fitted when the generalized Voellmy-like model was used. The fitting procedure required many trials because the two internal parameters influenced the two outputs x_{stop} and u_{obs} . To obtain the exact value of x_{stop} and/or u_{obs} , it was sometimes necessary to use many digits for the internal parameters μ_{max} or R . This means that outputs of this model do not vary continuously with internal parameters; in other words, there must be bifurcations in the relationship $\Omega = G(\Theta|\Pi, \text{path})$.

The range of variation of μ_{max} was 0.57 – 0.95; the range of variation of R was –0.79 to 4.45, when we consider all the events for both paths. There was only one negative value for R . For each avalanche, we also stored the values of the corresponding friction parameters $\xi(x)$ and $\mu(x)$ computed for the starting and stopping x -values of the path profile. The range of variation was wide, but consistent with the values reported in the literature. The starting values of ξ were sometimes higher than 10,000 m/s².

The two internal parameters used for the fitting appeared to be linearly independent (coefficient of determination $R^2=0.29$) when we combined the two paths (see Fig. 10). A distinction appears between Type 1 avalanches and the other types, more or less reproducing the separation already seen with the natural variables (Fig. 3). The data scattering for Type 1 avalanches is substantial compared to Types 2 and 3. Among others, regarding the mean of the internal parameters, there was not much difference between Type 1 to the two other types (see Table 4), whereas the standard deviations differed significantly. The correlation of the internal parameters with the input or output variables was negligible, except for the relationship between Z_{stop} and μ_{max} (coefficient of determination $R = 0.82$ or 0.95 according to the path, see Fig. 11); in this case, the data scattering results from the influence of the avalanche flow depth H . The other internal parameter R does not seem to depend on the path profile; it may genuinely reflect the dynamic behavior of the events.

In short, the generalized Voellmy-like model gave the expected results: all the events observed at the Lautaret Pass were reasonably well described. However, its use was less easy than the Voellmy-like model. It has *a priori* the substantial handicap of possessing six parameters. We explained earlier how we passed from six to only two parameters, in keeping μ_{min} , $\tan\theta_{moy}$ and the parameters of the relationship between $\xi(x)$ and $\mu(x)$ constant. All these parameters were the same for the Aulta and Lautaret paths, except for $\tan\theta_{moy}$ (0.25 versus 0.6). This parameter could be a regional parameter, but it is hard to believe that it can become a universal parameter. Finally, despite our efforts to minimize the number of parameters, this model has three parameters and this is probably too large to make it a convenient tool in the avalanche study.

6.3 The modified Coulomb-like model

All the events were fitted when the modified Coulomb-like model was used. To adjust the friction parameters, we first sought the values of μ by matching the computed and recorded distance for each event, then we altered the value of k for the avalanche to reach the recorded velocity. The fitting procedure was much simpler compared two other models. The values of μ fell within 0.49–0.68 and the values of k within 0.3–2.1. Moreover, the calculated velocities are shape-invariant (homothety) when \sqrt{k} varies (here \sqrt{k} varied from 0.54 to 1.5). For 11 events, this parameter was smaller than 1, whereas for 3 events it exceeded unity. This means that, if we set $k = 1$ (Coulomb model), the model can overestimate avalanche velocity.

Since the starting position was the same for all the events and the avalanche flow depth was not used in the computations, μ and Z_{stop} were found to be strongly linked; similarly, k and u_{obs} are linked together (see Fig. 12). Note that the two internal parameters reproduced the same separation between Type 1 avalanches and other avalanches, as shown previously (compare Fig. 13 and Fig. 3). The mean parameters of each group are given in Table 5. They clearly show that Type 1 avalanches went farther (μ is lower), with higher velocities (k is greater); the standard deviation was also larger for Type 1 avalanches. It is worth noting that all the values of k for the second group of avalanches (Types 2 and 3) did not exceed unity.

In short, when used as a conceptual model, this new model is an easy tool to simulate the motion of avalanches and gives good results when it is tested against field data coming from the Lautaret Pass database.

7 Conclusion

In this paper, the friction parameter of three conceptual models have been fitted by using field data obtained at the Lautaret Pass (14 events). For each event, we tried to linearly relate the input variables to the output variables, but we did not succeed. Consequently, we used nonlinear models based on the sliding-block analogy. We used two versions of the pervasive Voellmy model for the frictional force. For the first version, the two internal parameters are constant along the path profile; in the second version referred to as the generalized Voellmy-like model, they can vary along the path profile. For the third model, we proposed a new equation for the frictional force: a Coulombic (slope-dependent) contribution and a varying-mass effect, which involves replacing the mass m in the acceleration term by m/k , where k is a constant factor. The structure of this modified Coulomb-like model exhibits useful features.

Each of the three models has two parameters that have been fitted by using the data of 14 events. The main results can be summarized as follows:

- The Voellmy-like model fails when the measured velocities are high. Here only 50% of the events can be described by this model.
- The generalized Voellmy-like model has been constructed to offset this deficiency. The 14 events have been properly described. The model has six parameters and we set four of them by using *ad hoc* assumptions. These parameters are unlikely to be universal coefficients. Moreover, their fitting procedure is complicated.
- The modified Coulomb-like model is simple to use and the 14 events can be described properly. It is obviously the most appropriate model for the Lautaret Pass.

For the generalized Voellmy-like and modified Coulomb-like models, internal parameters can be partitioned into two groups, each corresponding to an avalanche family. Notably avalanches mobilizing powder snow go farther and reach higher velocities.

From the practical point of view, we can draw the following conclusions:

- Practitioners should be careful with the Voellmy model: this model is known to give good results for the run-out distance, but it can underestimate velocity. Consequently, it is better to use the modified Coulomb-like model. We can use $k = 1$ if there is no information regarding the nature of the avalanche. Table 5 provides values of k when the avalanche type is known.
- A conceptual model can be easily designed when data are available. In this case it can be an interesting alternative to a physically-based avalanche-dynamics model. So the crux of the issue turns around the availability of data.

References

- Ancey, C., 2004. Monte Carlo calibration of avalanches described as Coulomb fluid flows. *Philosophical Transactions of the Royal Society of London* (submitted).
- Ancey, C., Meunier, M., 2004. Estimating bulk rheological properties of flowing snow avalanches from field data. *Journal of Geophysical Research* 109, F01004.
- Bakkehoi, S., Cheng, T., Domaas, U., Lied, K., Perla, R., Schieldrop, B., 1980. On the computation of parameters that model snow avalanche motion. *Canadian Geotechnical Journal* 18, 1–10.
- Bakkehoi, S., Domaas, U., Lied, K., 1983. Calculation of snow avalanche run-out distance. *Annals of Glaciology* 4, 24–30.

- Bartelt, P., Salm, B., Gruber, U., 1997. Modelling dense snow avalanche flow as a Criminale-Ericksen-Filby fluid without cohesion. Tech. Rep. 717, SLF, Davos.
- Bon Mardion, G., Eybert-Beyrard, A., Guelff, C., Perroud, P., Rey, L., 1975. Mesures dynamiques dans l'avalanche. Résultats expérimentaux de la saison de neige 1973–1974. In: Colloque de la Société Hydrotechnique de France – section Glaciologie. Grenoble.
- Buser, O., Frutiger, H., 1980. Observed maximum run-out distance of snow avalanches and determination of the friction coefficients μ and ξ . *Journal of Glaciology* 26, 121–130.
- Dent, J., 1993. The dynamic friction characteristics of a rapidly sheared granular material applied to the motion of snow avalanches. *Annals of Glaciology* 18, 215–220.
- Eybert-Bérard, A., Mura, R., Perroud, P., Rey, L., 1977. La dynamique des avalanches. Résultats expérimentaux du Col du Lautaret. Année 1976. In: Colloque de la Société Hydrotechnique de France – section Glaciologie. Grenoble.
- Eybert-Bérard, A., Perroud, P., Brugnot, G., Mura, R., Rey, L., 1978. Mesures dynamiques dans l'avalanche - résultats expérimentaux du col du Lautaret (1972-1978). In: ANENA (Ed.), 2nde rencontre internationale sur la neige et les avalanches. Grenoble, pp. 203–224.
- Gubler, H., 1987. Measurements and modelling of snow avalanche speeds. In: *Avalanche formation, movement and effects*. Vol. 162. IAHS, Davos, pp. 405–420.
- Gubler, H., Hiller, M., Klausegger, G., Suter, U., 1986. Messungen an Fliesslawinen. Tech. Rep. 41. SLF, Davos.
- Harbitz, C., Issler, D., Keylock, C., 1998. Conclusions from a recent survey of avalanche computational models. In: Hestnes, E. (Ed.), 25 years of snow avalanche research. Vol. 203. Norwegian Geotechnical Institute, Voss, pp. 128–139.
- Meunier, M., Ancey, C., 2004. Towards a conceptual approach to predetermining high-return-period avalanche run-out distances. *Journal of Glaciology* (to be published).
- Mougin, P., 1922. Les avalanches en Savoie. Vol. IV. Ministère de l'Agriculture, Direction Générale des Eaux et Forêts, Service des Grandes Forces Hydrauliques, Paris.
- O'Connell, P. E., Todini, E., 1996. Modelling of rainfall, flow and mass transport in hydrological systems: an overview. *Journal of Hydrology* 175, 3–16.
- Perla, R., Cheng, T., McClung, D., 1980. A two-parameter model of snow-avalanche motion. *Journal of Glaciology* 26, 197–202.
- Salm, B., 1993. Flow, flow transition and runout distances of flowing avalanches. *Annals of Glaciology* 18, 221–226.
- Salm, B., Burkard, A., Gubler, H., 1990. Berechnung von Fliesslawinen, eine Anleitung für Praktiker mit Beispielen. Tech. Rep. No 47, Eidgenössischen Institut für Schnee- und Lawinenforschung (Davos).

- Savage, S., Hutter, K., 1989. The motion of a finite mass of granular material down a rough incline. *Journal of Fluid Mechanics* 199, 177–215.
- Schaerer, P., 1974. Friction coefficients and speed of flowing avalanches. In: *Symposium Mécanique de la Neige*. Vol. 114. IAHS, Grindelwald, pp. 425–432.



Figure 1: Photo of the avalanche paths equipped for experiments done in the 1970s and 1980s

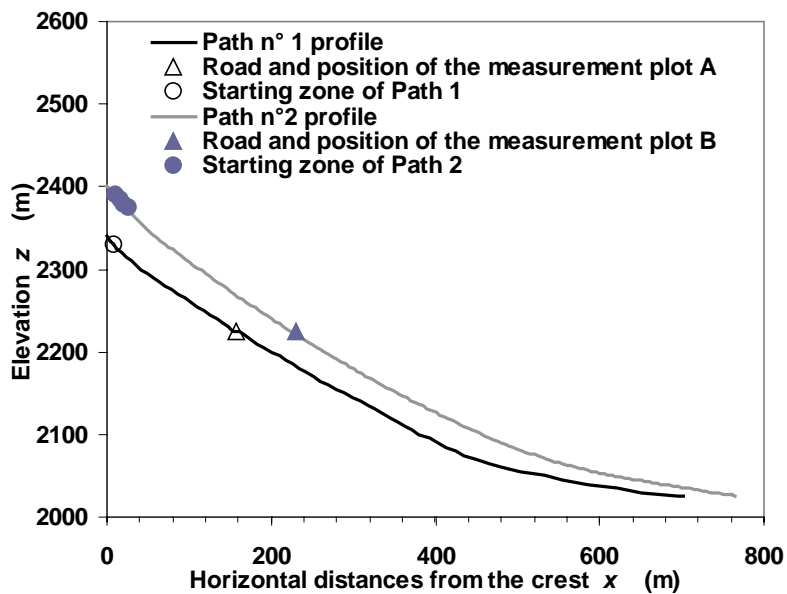


Figure 2: Path profiles n°1 and n°2 of the Col du Lautaret site

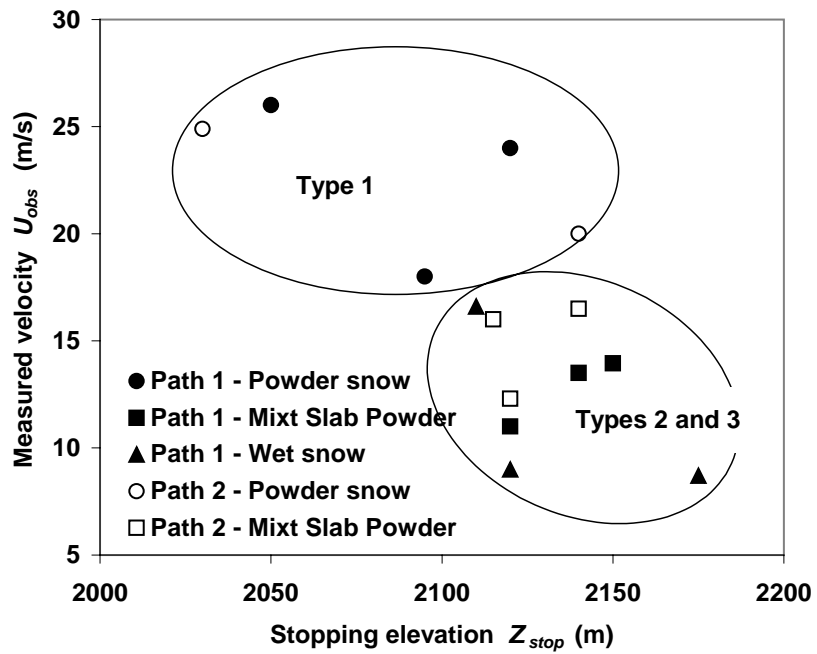


Figure 3: Separation between Type 1 avalanches and Types 2 and 3 avalanches.

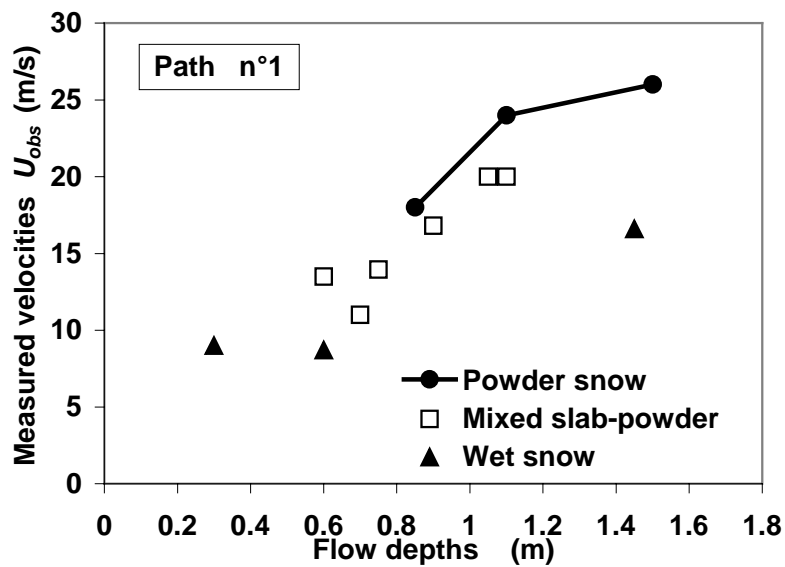


Figure 4: Relationship between the height and the velocity of the avalanche at the measurement point

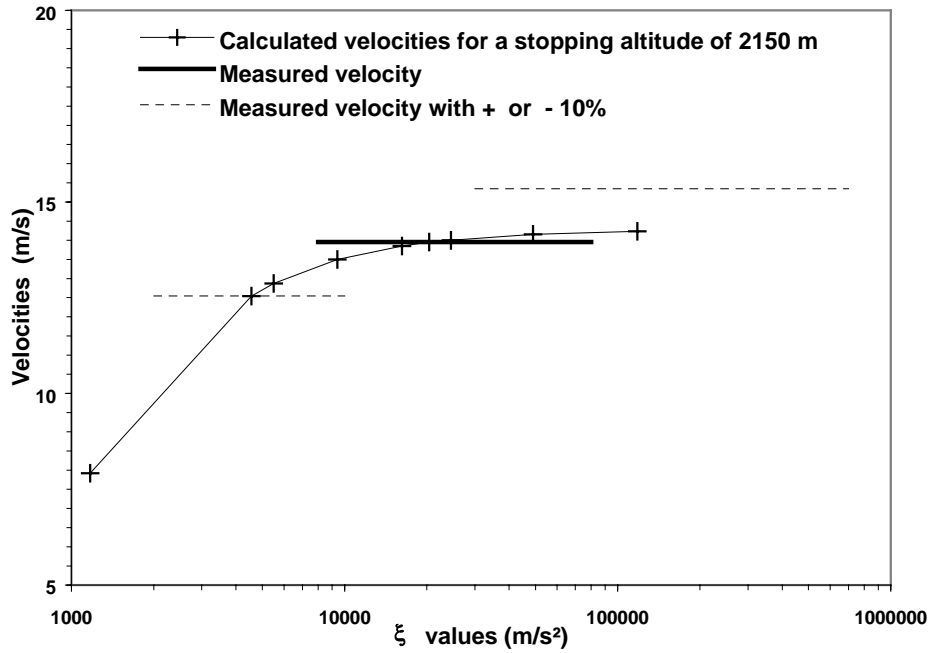


Figure 5: Results of the Voellmy-like model fitting for the event of 14/02/03 on Path 1, obtained for a fixed value of the stopping elevation

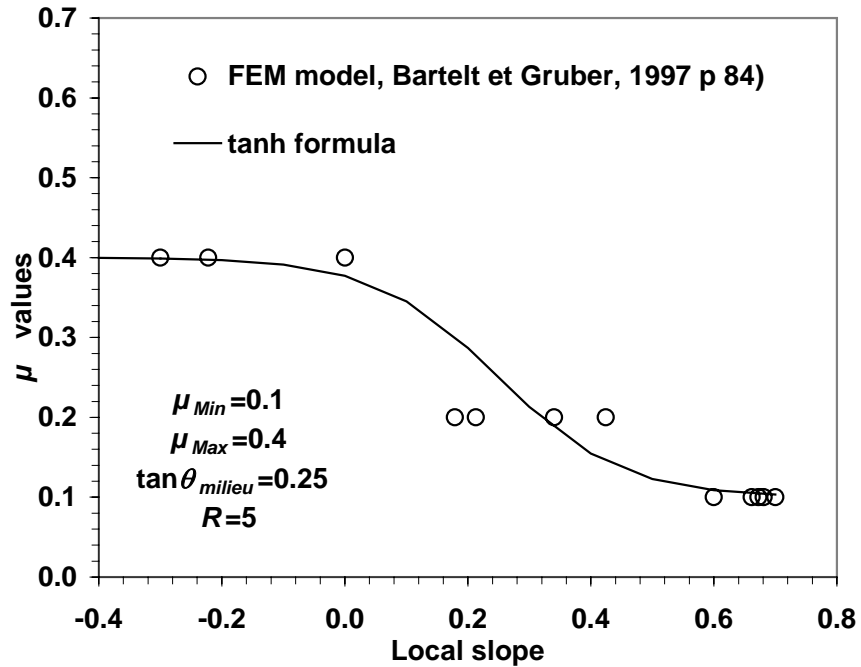


Figure 6: Relationship between μ values and the local slope for Aulta path (Bartelt and Gruber, 1997)

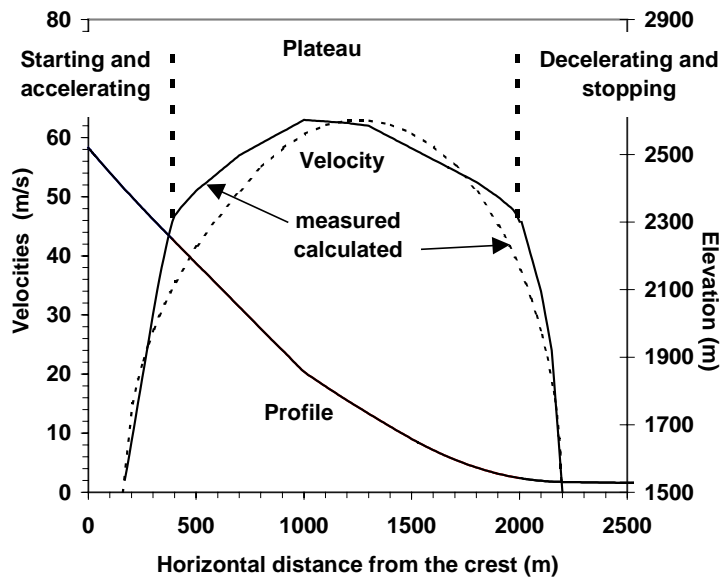


Figure 7: Profile of the Aulta avalanche dynamic with measured velocities (Bartelt and Gruber, 1997) and velocities calculated with the modified Coulomb-like model (dashed-line) ($\mu=0.4272$, $k=1.075$)

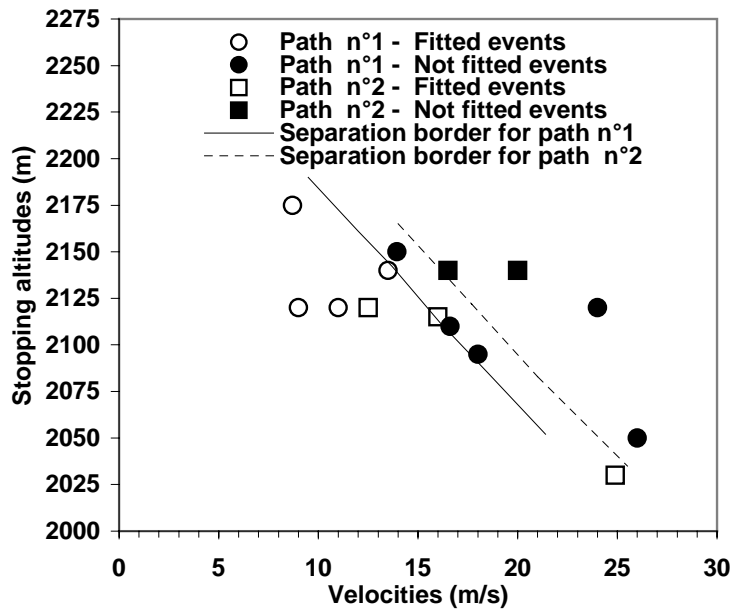


Figure 8: Separation between fitted events and nonfitted events for the Voellmy-like model

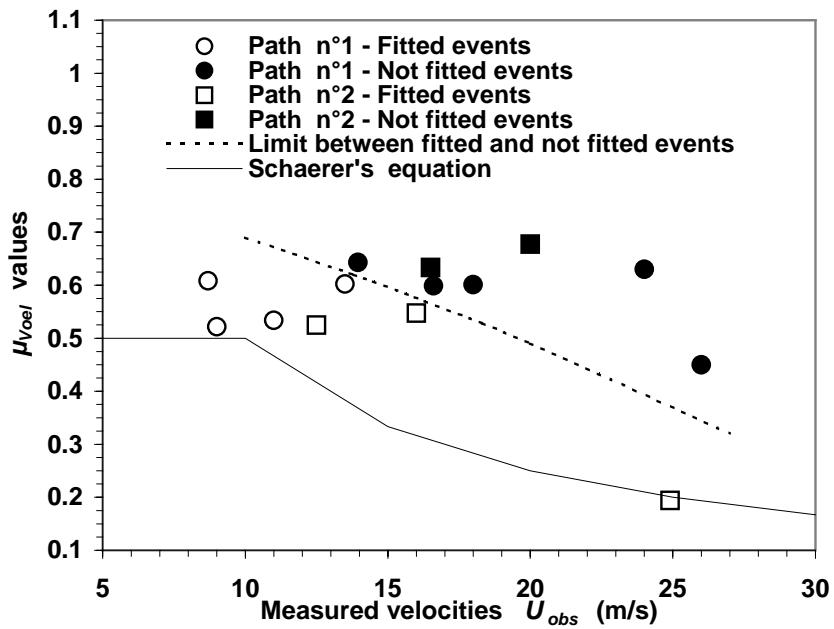


Figure 9: Results of the Voellmy-like model fitting on Col du Lautaret site data

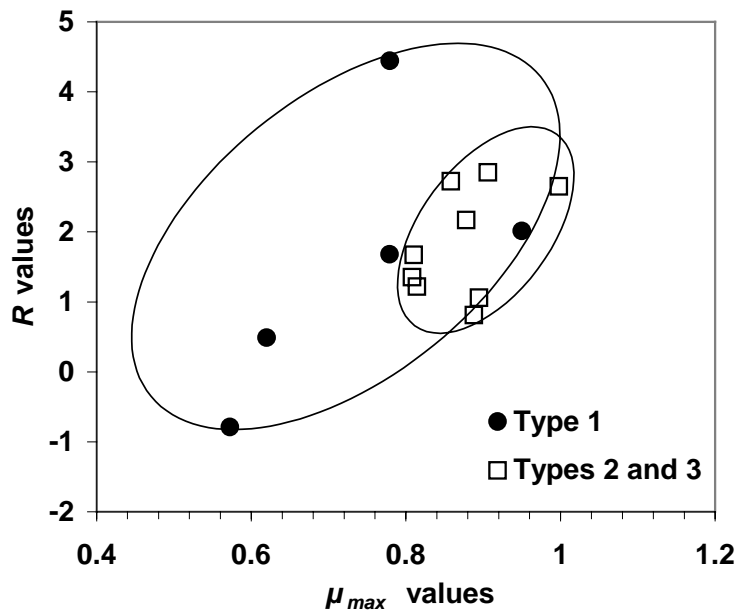


Figure 10: Independence between the two fitting parameters of the Generalized Voellmy-like model ($\mu_{min}=0.1 - \tan\theta_{moy}=0.6$)

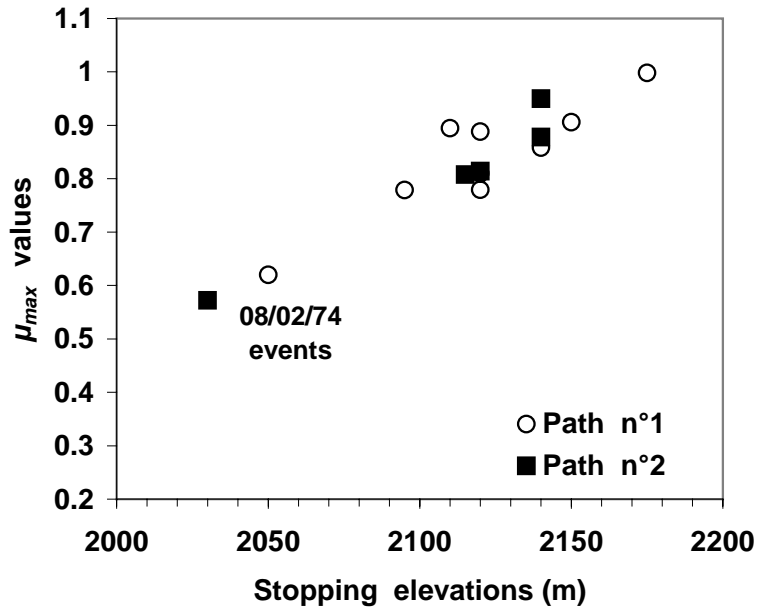


Figure 11: Variation of μ_{max} depending on the stopping elevation for Generalized Voellmy-like model

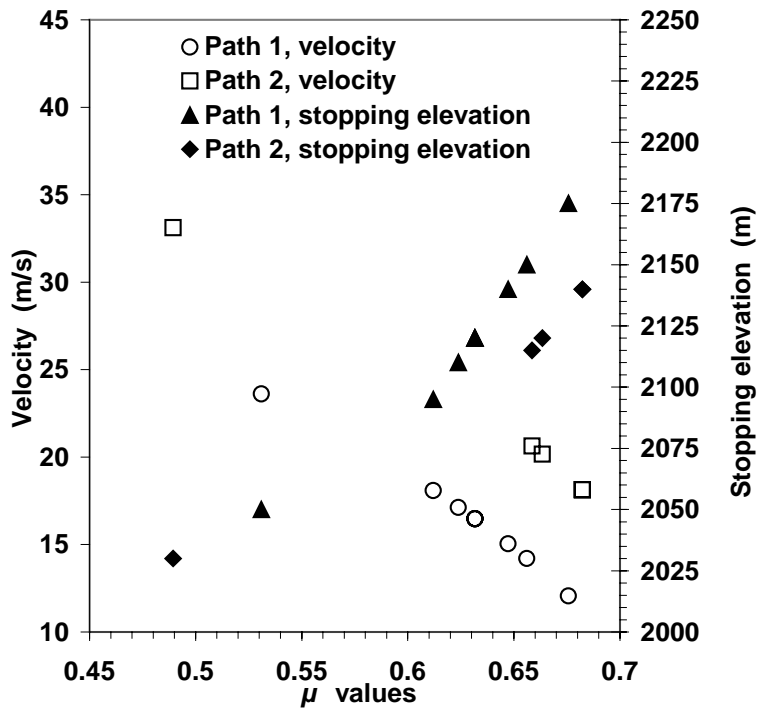


Figure 12: Relationship between the μ values of the modified Coulomb-like model and the stopping elevations and velocities for the Lautaret paths

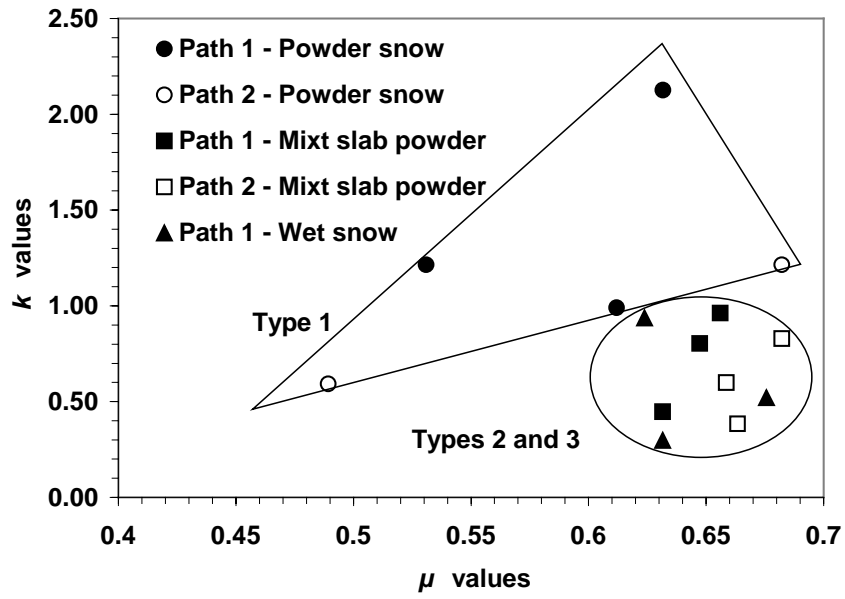


Figure 13: The internal parameters obtained by fitting the modified Coulomb-like model

Date	Avalanche type	x_{stop} (m)	z_{stop} (m)	Measured velocity (m/s)	Heights (m)	
					measured	used
24/01/1973	3	289	2150	10.35		
14/02/1973	3	289	2150	13.95	0.75	0.75
08/02/1974	4	532.75	2050	26	1.5	1.5
01/03/1974	3	345	2120	11	0.7	0.7
22/01/1975	2	309	2140	13.5	0.6	0.6
31/01/1975	2	362.75	2110		>1.3	1.3
12/03/1975	3			16.8	>0.9	0.9
17/02/1976	1	242.75	2175	8.7	0.6	0.6
08/12/1976	4	345	2120	24	1.1	1.1
23/02/1977	4	392.75	2095	18	0.85	0.85
27/01/1978	3			20	1.1	1.1
14/02/1978	3			20	1.05	1.05
29/03/1978	1	362.75	2110	16.6	>1.45	1.45
04/04/1978	1	345	2120	9	0.3	0.3

a) Path no. 1

Date	Avalanche type	x_{stop} (m)	z_{stop} (m)	Measured velocity (m/s)	Heights (m)	
					measured	used
24/01/1973	3	430.4	2110			
14/02/1973	3	372.0	2140	16.5	0.8	0.8
08/02/1974	4	738.3	2030	24.9	>1	1
22/01/1975	2	421.1	2115	16	0.7	0.7
12/03/1975	3			16.5	>0.84	0.84
06/02/1976	4	372.0	2140	20	1.5	1.5
17/02/1976	2	411.6	2120	12.5	0.5	0.5
04/04/1978	1	430.4	2110		>1.5	1.5

b) Path no. 2

Table 1: Usable data on Col du Lautaret site

Number of the category	Avalanche type	Nature of the snow	Density (kg/m ³)
1	Powder snow	Cold, dry	80-120
2	Mixed slab-powder	Cold, dry	120-250
3	Wet snow	Snow at 0°C, wet	250-400

Tableau 2: Avalanche and snow types (Eybert-Beyrard A. et al., 1978): “powder snow” does not mean that the avalanche was airborne but that the avalanche mobilized powder snow. “Cold” means that temperature is below 0°C.

Success or failure of the fitting	Avalanche type		Total
	1	2 and 3	
Success	1	6	7
Failure according to $u_{obs} < 0.9 * u_{asympt}$	2	2	4
Failure according to $u_{obs} < u_{asympt}$	1	2	3
Total	4	10	14

Table 3: Results of fitting the Voellmy-like model

Avalanche type	Mean value	Standard deviation
μ_{max}		
Type 1	0.74	0.15
Types 2 and 3	0.87	0.06
R		
Type 1	1.57	1.95
Types 2 and 3	1.83	0.78

Table 4: Results of fitting the Generalised Voellmy-like model, for $\mu_{min} = 0.1$ and $\tan\theta_{moy} = 0.6$

Avalanche type	Mean value	Standard deviation
μ_{Coul}		
Type 1	0.59	0.08
Types 2 and 3	0.65	0.02
k		
Type 1	1.23	0.56
Types 2 and 3	0.64	0.25

Table 5: Results of fitting the modified Coulomb-like model